Materials Research. 2017; 20(4): 874-881
DOI: http://dx.doi.org/10.1590/1980-5373-MR-2016-0670

Study of the Nanostructure Effect on Polyalkylthiophene Derivatives Films Using Impedance Spectroscopy

Lucas Vinicius de Lima Citolino[a], Maria Luisa Braunger[a], Vinícius Jessé Rodrigues Oliveira[a], Clarissa A. Olivati[a]*

[a] *Faculdade de Ciências e Tecnologia, Universidade Estadual Paulista, CP 467, 19060-900 Presidente Prudente, SP, Brazil*

Received: September 15, 2016; Revised: January 06, 2017; Accepted: February 18, 2017

In this paper, devices fabricated with a diode-like structure (electrode/polymer/electrode) from spin-coated and nanostructured (Langmuir-Schaefer) films of polythiophene derivatives were characterized by impedance spectroscopy and studied by theoretical fitting to reach a better understanding of the physical processes in the devices. The materials used for this research were the polyalkylthiophene (P3AT) derivatives poly(3-butylthiophene) (P3BT), poly(3-hexylthiophene) (P3HT), poly(3-octylthiophene) (P3OT) and poly(3-decylthiophene) (P3DT). Electrical measurements were performed from 1 Hz to 1 MHz (100 mV ac) while increasing the dc bias in the range from 0 to 2.5 V. The fittings of the experimental results were performed using equivalent circuits. By plotting the theoretical and experimental spectra on a single graph, it was possible to obtain information related to the film morphology, interfacial effects, resistance, capacitance and conductivity of the polymer, thereby enhancing the understanding of this particular type of device. Among the P3AT films, those grown by the Langmuir-Schaefer technique showed higher electrical conductivity, with the only exception being that of P3BT.

Keywords: *polythiophene, nanostructured film, impedance spectroscopy*

1. Introduction

Polythiophenes have been a particular focus among conventional conductors due to their good stability and easy processability[1,2]. In some reports, attention has been paid to regioregular polyalkylthiophene derivatives (P3AT), where the increased alkyl chain length of the polymer increases its solubility, a property that is extremely important for the production of high-quality organic electronic devices[2,3]. In organic electronics, P3AT thin films offer a number of applications, such as in light-emitting diodes, sensors and solar cells[4–9]. The thin films can be fabricated by deposition techniques such as spin-coating, Langmuir-Blodgett (LB) and Langmuir-Schaefer (LS)[10–12].

Impedance spectroscopy analysis has proven to be a useful technique to study the electrical properties of devices built from thin films of semiconductor materials[13]. The technique consists of measuring the complex impedance (Z^*) over a wide frequency range (f)[12,14]. From the spectrum of Z^* *vs.* f, relevant information can be obtained, such as the bulk conductivity, as well as data on the interface between the electrode and materials, such as the injection and charge accumulation[15]. One analysis tool is theoretical models based on equivalent circuits that can adequately explain the results obtained from the impedance spectra[14–16]. This is a simple way to describe the features of structures containing an active layer between two electrodes, by using elements in the circuit[17].

The present study addresses the influence of the thin film deposition technique as applied to P3AT derivatives as measured by impedance spectroscopy. The LS technique provides nanostructured thin films, and it was compared herein to the widely used spin-coating technique. The transport mechanisms of the charge carriers were evaluated through impedance spectroscopy results for different P3AT derivatives and morphologies. The interfacial electrical features of the devices were analyzed by the theoretical modeling of the experimental results.

2. Materials and Methods

The materials used for this study were the P3AT derivatives poly(3-butylthiophene) (P3BT), poly(3-hexylthiophene) (P3HT), poly(3-octylthiophene) (P3OT) and poly(3-decylthiophene) (P3DT), all obtained from Sigma-Aldrich. Regarding the regioregularity, the values found for the P3BT, P3HT, P3OT and P3DT were approximately 80 – 90%, ≥ 90%, ≥ 90 %, 98.5%, respectively. The polymers were used as thin films deposited by the spin-coating and LS techniques onto ITO (indium-tin oxide) substrates (Delta Technology), which has an average covered area of 1.6 cm^2 and the sheet resistance (Rs) between 5 and 15 Ω.

The spin-coating technique is used to fabricate thin films onto plain substrates. A spinner was used for the

* e-mail: olivati@fct.unesp.br

production of the thin films, with rotation speed of 1000 rpm for 60 seconds. The P3AT derivatives were dissolved in chloroform in solutions of 15 mg/ml, except P3BT which had a concentration of 10 mg/ml due to the difficulty to solubilize this material in large quantities[18].

A LS film is made of one or more layers of stabilized Langmuir film by a horizontal contact of the substrate with the monolayer at constant surface pressure (SP) followed by a slowly lift of the substrate. For the LS films, the P3AT derivatives were dissolved also in chloroform, however in solutions with concentration of 0.2 mg/ml. The P3BT derivative was deposited in SP = 30 mN/m, while the derivatives P3HT, P3OT and P3DT were deposited in SP = 20 mN/m[18].

The thicknesses of the films were determined by a Veeco Dektak 150 profilometer. The thicknesses of the P3AT films obtained by profilometry measurements for P3BT, P3HT, P3OT and P3DT were approximately 101, 129, 96 and 133 nm for the spin-coated films and 71, 317, 233 and 220 nm for the LS films, respectively. The numbers of deposited layers were 10, 25, 25 and 15 for the P3BT, P3HT, P3OT and P3DT films, respectively. Aluminum (Al) electrodes were deposited onto the P3AT films by physical vapor deposition using an Edwards 306 Auto Evaporation System, forming a diode-like structure of ITO/P3AT/Al.

The electrical measurements were carried out using a Solartron impedance analyzer, mod. 1260A. The amplitude of the ac signal applied was 100 mV, and the frequency (*f*) ranged from 1 to 10^6 Hz. A superposed dc bias was applied to the ac signal, from 0 to 2.5 V. The results were analyzed by the impedance spectra: imaginary impedance (-*Z*") versus real impedance (*Z*'), -*Z*" versus *f* and *Z*' versus *f*. From the impedance spectra were obtained the parameters for the equivalent electrical circuits used in the theoretical modeling.

The theoretical models were proposed using equivalent electrical circuits of associated resistors and capacitors. The resistors are used to represent the possible resistance of the materials or the interface resistance between two different materials. The capacitors, on the other hand, are used to represent the charge accumulation at the interfaces, thus defining the characteristic relaxation times of the studied structures. The theoretical model applied was the equivalent circuit (equation (1))[17], in which the α parameter analytically simulates the distribution of the dielectric relaxation time τ, where $0 \leq \alpha \leq 1$.

$$Z^* = R + \frac{R_1}{1+(\omega R_1 C_1)^{1-\alpha_1}} + \frac{R_2}{1+(\omega R_2 C_2)^{1-\alpha_2}} + \left(\frac{R_1}{1+(\omega R_1 C_1)^{1-\alpha_1}} + \frac{R_2}{1+(\omega R_2 C_2)^{1-\alpha_2}}\right) j \quad (1)$$

The model provides a symmetric distribution of the relaxation times and facilitates the development of more complex models. Applying Mathcad software version 14.0, the analysis of the experimental data and the theoretical modeling of the electrical measurements were performed.

The electrical conductivity of the materials was calculated from the equation (2), where *l* is the film thickness (in nm), *A* is the effective area of the device (in cm^2) and *R* the resistance of the material used (in Ω).

$$\sigma = \frac{1}{R} \cdot \frac{l}{A} \quad (2)$$

3. Results and Discussion

The *Z*' *vs. f* plots obtained for the ITO/P3AT/Al devices, in which the P3AT films were deposited by the spin-coating (ITO/P3AT(spin-coating)/Al) and LS (ITO/P3AT(LS)/Al) techniques, are shown in Figure 1. The experimental results are represented by open symbols, while the different types of lines are the theoretical fittings. Through these results, one can see some similarities between the spectra of the devices.

In the *Z*' *vs. f* data, there is a behavior where *Z*' tends to reach constant values (plateaus) at low and high frequencies. This is a clear result for some plots, as for the P3HT spin-coated film at low frequencies, but it is not evident for others, and this justifies the use of theoretical fitting. The plateaus shift at low frequencies according to the dc bias applied. This result is possibly related to the reduction of the potential barrier at the Al/P3AT interface when the applied dc bias increases[17].

Figure 2 shows the -*Z*" *vs. f* plots obtained for ITO/P3AT/Al devices in which the P3AT films were deposited by spin-coating (ITO/P3AT(spin-coating)/Al) and LS (ITO/P3AT(LS)/Al) techniques. As for the *Z*' *vs. f* plots, the experimental results are represented by open symbols, while the different types of lines are the theoretical fittings.

In the -*Z*" *vs f* spectra, for the spin-coated and LS films of P3BT, there can be observed one well-defined relaxation peak that shifts to lower frequencies with the increase in the dc bias applied. For the P3HT spin-coated film, there is only one relaxation peak that shifts in the middle frequencies, while the P3HT LS film presents two relaxation peaks, one that shifts from low to medium frequencies (approximately 10 to 10^2 Hz) and the other, less defined, remains constant at high frequencies. For the spin-coated and LS films of P3OT, there is only one well-defined relaxation peak formed, similar to the P3BT case. However, it is possible to observe the formation of a shoulder peak at approximately 10^4 Hz for the P3OT LS film. For the spin-coated and LS films of P3DT, there may be observed one well-defined relaxation peak at low frequencies and one shoulder peak at higher frequencies. The shoulder peaks improve their definition with the applied dc bias.

Some plateaus and relaxation peaks can only be observed due to the extrapolation of the frequency used in the theoretical fittings. Argand diagrams for devices in which derivatives of P3AT have been deposited by spin-coating and LS are shown in Figure 3 and Figure 4, respectively. In the Argand diagram for the ITO/P3AT/Al devices, it is possible to observe only one semicircle, which is possibly due to the overlapping of

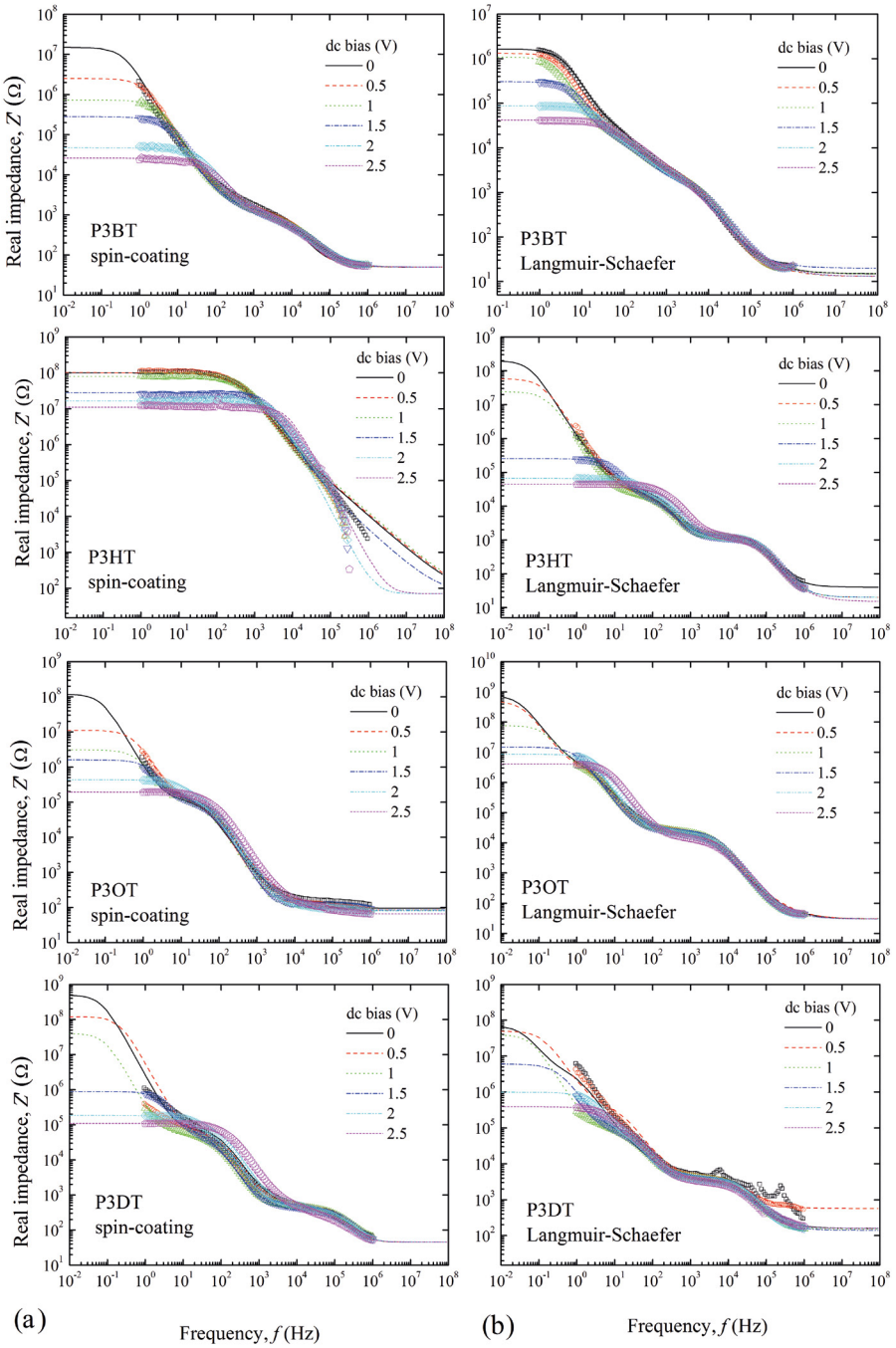

Figure 1. *Z' vs.* f plots for ITO/P3AT/Al devices containing a) spin-coated and b) LS films. The experimental results are represented by open symbols.

two or more semicircles. In all diagrams, *Z** tends to form smaller semicircles upon increasing the dc bias voltage, wherein the diameter of the semicircle is related to the total resistance of the device[19]. In the theoretical fittings, each circle shall be related to an RC circuit in parallel.

The experimental data were analyzed using the electrical circuits shown in Figure 5. For the devices of the P3AT spin-coated films, an equivalent circuit was used containing two parallel RC (Figure 5(a)), except for P3DT, and for the P3AT LS films, the equivalent circuit contained three parallel RC (Figure 5(b)). Due to the higher roughness, the P3AT films deposited by LS have more contact surface with the aluminum electrode, which may cause greater interfacial effects. This is a possible explanation for the additional

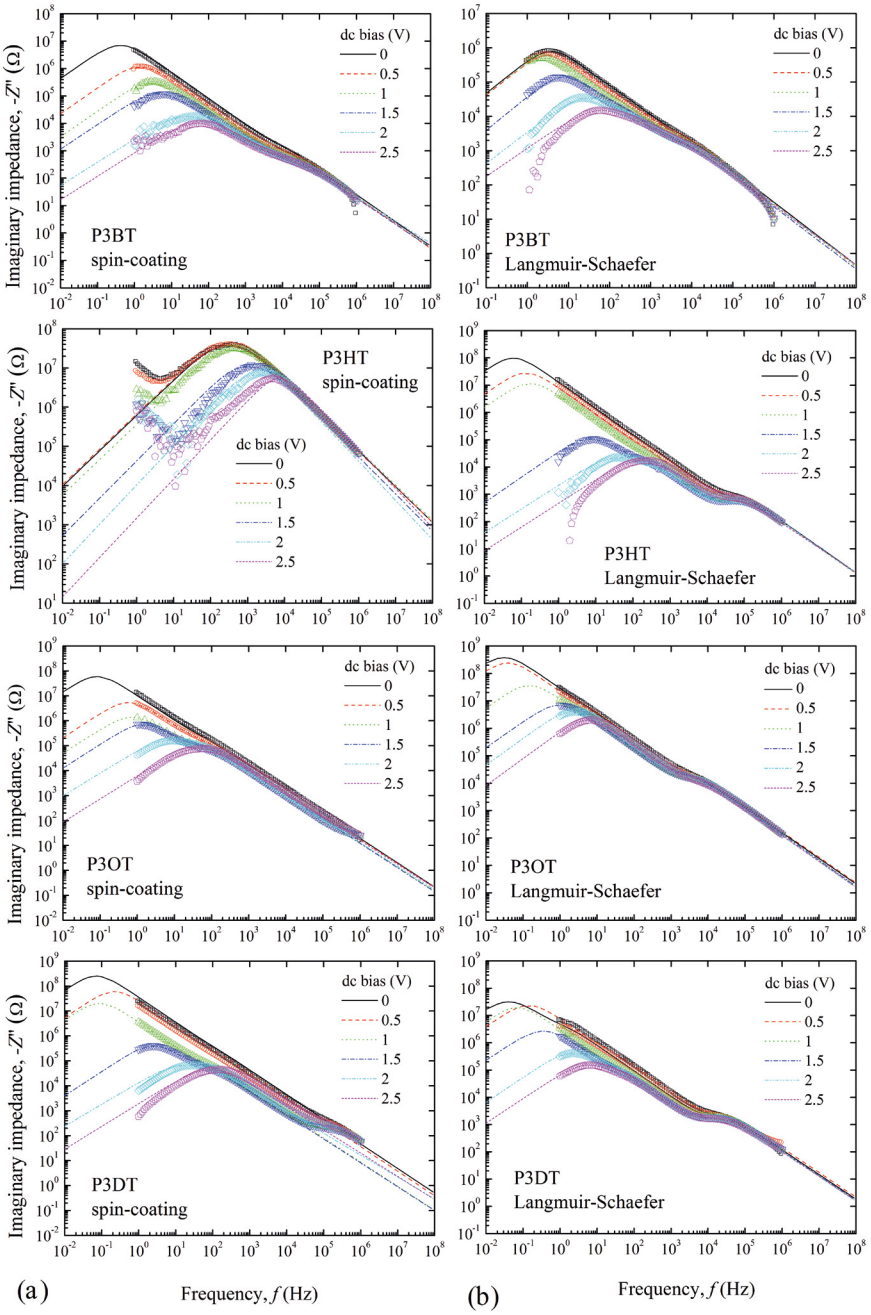

Figure 2. *-Z'' vs.* f plots for ITO/P3AT/Al devices containing a) spin-coated and b) LS films. The experimental results are represented by open symbols.

parallel RC circuit required in the theoretical fitting for the ITO/P3AT(LS)/Al devices.

Through theoretical fittings of the Argand diagrams, for most devices in which the P3AT derivatives were deposited by the spin-coating technique, it is possible to evaluate the superposition of two semicircles. Only for the ITO/P3DT(spin-coating)/Al device did the theoretical fitting show the superposition of three semicircles. As for the ITO/P3AT(spin-coating)/Al devices, the ITO/P3AT(LS)/Al devices also exhibited only one semicircle, but in this case, it was due to the superposition of three semicircles. Table 1 shows the parameters obtained by fittings performed on the experimental curves shown in impedance spectra at a dc bias of 0 V.

Using the equivalent circuit obtained from the analysis of the experimental and theoretical spectra and the results of

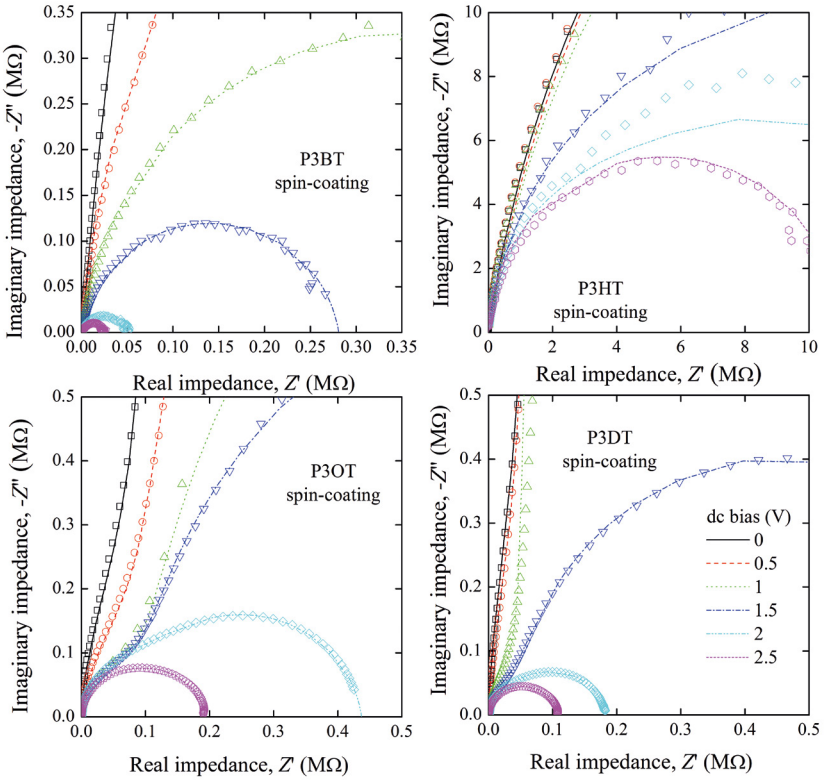

Figure 3. Argand diagrams for the ITO/P3AT(spin-coating)/Al devices. The experimental results are represented by open symbols.

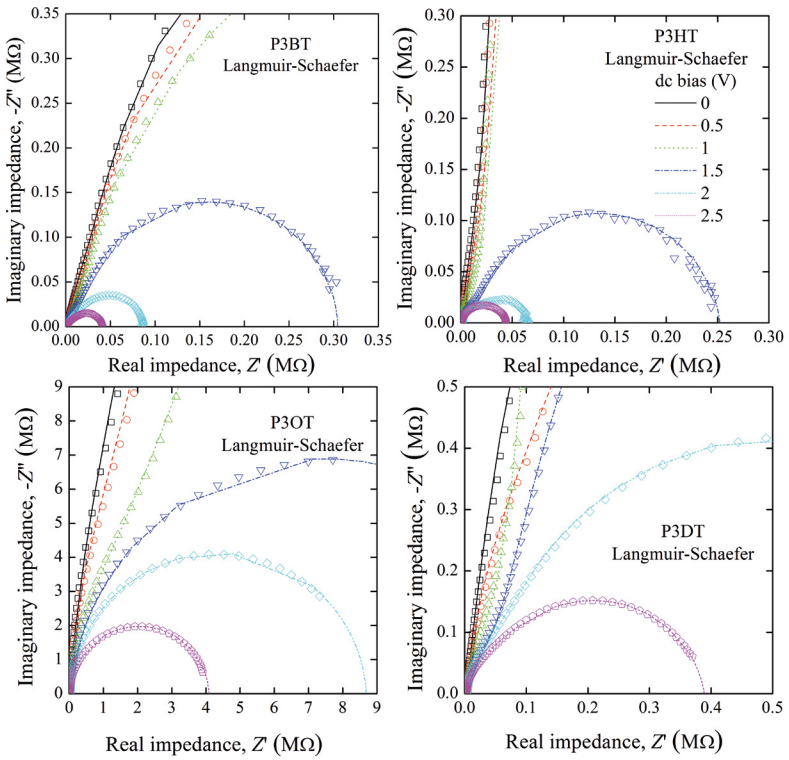

Figure 4. Argand diagrams for the ITO/P3AT(LS)/Al devices. The experimental results are represented by open symbols.

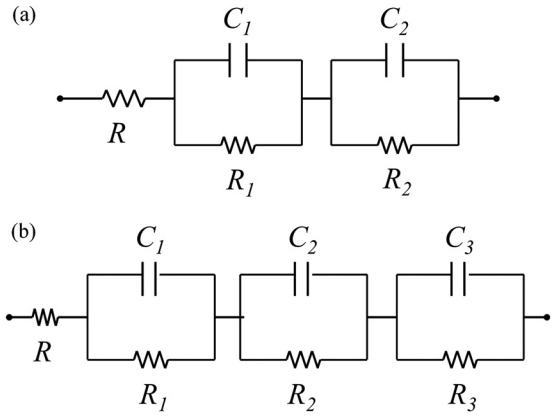

Figure 5. Equivalent electrical circuits used in the theoretical fitting for the ITO/P3AT/Al devices.

Table 1, for the ITO/P3AT(spin-coating)/Al devices there can be identified i) one parallel circuit R_1C_1 (~10^4 Hz), wherein R_1 and C_1 are the resistance and capacitance of the bulk of the polymer (P3AT), ii) one parallel circuit R_2C_2 (at low frequency), wherein R_2 and C_2 represent the values at the P3AT(spin-coating)/Al interface and iii) one resistance R, representing the resistance of the P3AT(spin-coating)/ITO interface (ohmic contact). The ITO/P3DT(spin-coating)/Al device showed an additional RC circuit, R_3C_3. For the ITO/P3AT(LS)/Al devices, there can be identified i) one parallel circuit R_1C_1 (~10^4 Hz), wherein R_1 and C_1 are the resistance and capacitance of the bulk of the polymer (P3AT), ii) two parallel circuits (both at low frequency), R_2C_2 and R_3C_3, wherein R_2, R_3, C_2 and C_3 represent the values at the P3AT(LS)/Al interface and iii) one resistance R, representing the resistance at the P3AT(LS)/ITO interface (ohmic contact).

To realize the theoretical fittings from the equivalent electrical circuits in impedance measurements for a device, such as an ITO/doped organic layer/Ag, Chen *et al.*[16] used an equivalent electrical circuit consisting of two RC circuits in parallel and one series resistance. The Argand diagrams showed two semicircles, and the spectra of *Z' vs. f* showed a tendency to form two plateaus. The semicircles and plateaus were related to the RC circuits, where one circuit represents the resistance and capacitance of the doped organic layer/Ag interface and the other represents those of the doped organic layer. The series resistance was correlated with the ITO/organic layer doped interface.

Studies using the impedance technique performed by Olivati *et al.*[17] on polymer light-emitting devices (PLEDs) fabricated from poly(2-methoxy-5-hexyloxy)-p-phenylenevinylene (OC_1OC_6–PPV) thin films by the LB technique and the structure ITO/OC_1OC_6–PPV(LB)/Al reported that the spectrum of *Z' vs f* presented two plateaus. The measurements were fitted by an equivalent circuit composed of two parallel RC circuits with a series resistance, and through the values obtained by the theoretical fittings, it was identified that one RC circuit represents the resistance and capacitance of the OC_1OC_6–PPV(LB) layer, the other represents the OC_1OC_6–PPV(LB)/Al interface, and the series resistance represents the ITO/OC_1OC_6–PPV(LB) interface.

Mirsky *et al.*[20], using impedance spectroscopy, reported information on the resistance of the polymer and metal/polymer interface of a thin film of polypyrrole-deposited gold electrodes. The spectrum of *-Z'' vs. Z'* was fitted by an equivalent circuit having a series resistance connected to three RC circuits in parallel. One RC circuit represents the resistance and the capacitance of the electrode/polymer interface, and the other two represent the capacitance and the resistance of the bulk of the conductive polymer.

Table 2 shows the electrical conductivities for the devices of P3AT spin-coated and LS films obtained from equation (2). In general, the LS films showed higher electrical conductivity than the spin-coated films. The LS film of P3HT showed a higher electrical conductivity (order of 10^{-5} S/m) that any of the other derivatives. A factor related to the highest conductivity is the mobility of charge carriers because P3HT has the highest regioregularity. Charge carriers and excitons can move along its longer connected chains, enable more jumps to neighboring chains[21,22]. The side chain length is also a factor that affects the mobility of charge carriers, because with increasing alkyl side chain length, P3AT thin films showed a decreased number of

Table 1. Parameters obtained through the theoretical fittings of components *Z'* and *Z''* by Eq. 1 for the ITO/P3AT(spin-coating)/Al and ITO/P3AT(LS)/Al devices.

	Deposition technique	R1 (Ω)	C1 (F)	R2 (Ω)	C2 (F)	R3 (Ω)	C3 (F)	R (Ω)
P3BT	spin-coating	$1x10^3$	$1.2x10^{-7}$	$1.5x10^7$	$1.6x10^{-7}$	-	-	50
P3BT	LS	$2.6x10^4$	$3.6x10^{-7}$	$2.1x10^3$	$1.1x10^{-7}$	$1.6x10^6$	$1.6x10^{-7}$	15
P3HT	spin-coating	$4x10^7$	$3.6x10^{-11}$	$6.1x10^7$	$8.6x10^{-11}$	-	-	70
P3HT	LS	$1.05x10^3$	$1.3x10^{-8}$	$1.9x10^4$	$3.6x10^{-7}$	$2x10^8$	$8.2x10^{-8}$	40
P3OT	spin-coating	$1x10^5$	$2.2x10^{-7}$	$1.2x10^8$	$1x10^{-7}$	-	-	95
P3OT	LS	$1.6x10^4$	$1.6x10^{-8}$	$2.5x10^6$	$1.8x10^{-7}$	$8x10^8$	$4.1x10^{-8}$	30
P3DT	spin-coating	$7x10^4$	$1.4x10^{-7}$	$4x10^2$	$1.6x10^{-8}$	$5x10^8$	$2.8x10^{-8}$	45
P3DT	LS	$3x10^3$	$1.4x10^{-8}$	$3x10^6$	$2.8x10^{-7}$	$7x10^7$	$3.5x10^{-7}$	160

Table 2. Electrical conductivity values for thin films of P3AT derivatives deposited by spin-coating and LS.

Deposition	Polymer	Conductivity (S/m)
spin-coating	P3BT	$8.4x10^{-6}$
LS	P3BT	$2.3x10^{-7}$
spin-coating	P3HT	$2.7x10^{-10}$
LS	P3HT	$2.5x10^{-5}$
spin-coating	P3OT	$8x10^{-8}$
LS	P3OT	$1.2\ x10^{-6}$
spin-coating	P3DT	$1.6x10^{-7}$
LS	P3DT	$6.1x10^{-6}$

ordered structures, thus hampering the transport of charge carriers in the semiconductor and at the interface between the semiconductor and electrodes[23].

Unlike other P3AT derivatives, the P3BT thin film deposited by spin-coating showed a higher electrical conductivity compared to that deposited by LS. The films deposited by the LS technique generally showed a higher electrical conductivity, probably due to the organization at the molecular level that can be provided by Langmuir techniques[24,25]. However, the P3BT presented a less efficient adhesion onto the ITO substrate when compared with the other P3AT derivatives. Thus, it is possible that the deposition issues influenced the layer packaging, thus hampering the mobility of charge carriers and decreasing the electrical conductivity of the LS film for P3BT.

4. Conclusions

In summary, the theoretical modeling of the equivalent electrical circuit has been shown to be an important tool for analysis of impedance spectroscopy measurements. The theoretical model used satisfactorily simulates the data obtained for the ITO/P3AT/Al devices. With the analysis of the experimental/theoretical spectra and the values of the parameters used in the equivalent electric circuit, information was obtained and related to electronic transport properties and interfacial effects.

For the polymers P3BT, P3HT and P3OT in the ITO/P3AT/Al structure, the theoretical fit shows that the films deposited by spin-coating could be fitted by two parallel RC, and those deposited by LS should be fitted by three parallel RC. The only exception is P3DT, which was fitted by three parallel RC regardless of the deposition technique used to build the thin film. Among the P3AT films, those grown by the LS technique showed a higher electrical conductivity than those deposited by spin-coating probably related to the distinct molecular arrangement provided by the deposition technique, with the only exception being P3BT. For LS films, the conductivity was found to decrease with increasing of alkyl chain length.

5. Acknowledgments

The authors are grateful for the financial support of the Brazilian agencies FAPESP, INEO/CNPq and CAPES.

6. References

1. Bao Z, Dodabalapur A, Lovinger AJ. Soluble and processable regioregular poly(3-hexylthiophene) for thin film field-effect transistor applications with high mobility. *Applied Physics Letters*. 1996;69(26):4108-4110. DOI: 10.1063/1.117834.

2. Boman M, Stafström S, Brédas JL. Theoretical investigations of the aluminum/polythiophene interface. *Journal of Chemical Physics*. 1992;97(12):9144-9153. DOI: 10.1063/1.463340.

3. Babel A, Jenekhe SA. Alkyl chain length dependence of the field-effect carrier mobility in regioregular poly(3-alkylthiophene) s. *Synthetic Metals*. 2005;148(2):169-173. DOI: 10.1016/j.synthmet.2004.09.033.

4. Bai H, Shi G. Gas sensors based on conducting polymers. *Sensors (Basel)*. 2007;7(3):267-307.

5. Yu G, Gao J, Hummelen JC, Wudl F, Heeger AJ. Polymer Photovoltaic Cells: Enhanced Efficiencies Via a Network of Internal Donor-Acceptor Heterojunctions. *Science*. 1995;270(5243):1789-1791. DOI: 10.1126/science.270.5243.1789.

6. Ohshita J, Tada Y, Kunai A, Harima Y, Kunugi Y. Hole-injection properties of annealed polythiophene films to replace PEDOT-PSS in multilayered OLED systems. *Synthetic Metals*. 2009;159(3-4):214-217. DOI: 10.1016/j.synthmet.2008.09.002.

7. Chang JB, Liu V, Subramanian V, Sivula K, Luscombe C, Murphy A, et al. Printable polythiophene gas sensor array for low-cost electronic noses. *Journal of Applied Physics*. 2006;100(1):014506. DOI: 10.1063/1.2208743.

8. McNeill CR, Halls JJM, Wilson R, Whiting GL, Berkebile S, Ramsey MG, et al. Efficient Polythiophene/Polyfluorene Copolymer Bulk Heterojunction Photovoltaic Devices: Device Physics and Annealing Effects. *Advanced Functional Materials*. 2008;18(16):2309-2321. DOI: 10.1002/adfm.200800182.

9. Clarke TM, Ballantyne AM, Nelson J, Bradley DDC, Durrant JR. Free Energy Control Of Charge Photogeneration in Polythiophene/Fullerene Solar Cells: The influence of Thermal Annealing on P3HT/PCBM Blends. *Advanced Functional Materials*. 2008;18(24):4029-4035. DOI: 10.1002/adfm.200800727.

10. Zribi A, Fortin J, eds. *Functional Thin Films and Nanostructures for Sensors: Synthesis, Physics, and Application*. New York: Springer; 2009. DOI: 10.1007/b138612.

11. Sanfelice RC, Gonçalves VC, Balogh DT. Langmuir and Langmuir-Schaefer Films of Poly(3-hexylthiophene) with Gold Nanoparticles and Gold Nanoparticles Capped with 1-Octadecanethiol. *The Journal of Physical Chemistry C*. 2014;118(24):12944-12951. DOI: 10.1021/jp503083k.

12. Jayaraman S, Yu LT, Srinivasan MP. Polythiophene-gold nanoparticle hybrid systems: Langmuir-Blodgett assembly of nanostructured films. *Nanoscale*. 2013;5(7):2974-2982. DOI: 10.1039/C3NR33385J.

13. Johnson BW, Read DC, Christensen P, Hamnett A, Armstrong RD. Impedance characteristics of conducting polythiophene films. *Journal of Electroanalytical Chemistry*. 1994;364(1-2):103-109. DOI: 10.1016/0022-0728(93)02923-6.

14. Barsoukov E, Macdonald JR, eds. *Impedance Spectroscopy: Theory, Experiment, and Appplications*. Hoboken: John Wiley & Sons; 2005. 616 p.

15. Chinaglia DL, Gozzi G, Alfaro RAM, Hessel R. Espectroscopia de impedância no laboratório de ensino. *Revista Brasileira de Ensino de Física*. 2008;30(4):4504.

16. Chen CC, Huang BC, Lin MS, Lu YJ, Cho TY, Chang CH, et al. Impedance spectroscopy and equivalent circuits of conductively doped organic hole-transport materials. *Organic Electronics*. 2010;11(12):1901-1908. DOI: 10.1016/j.orgel.2010.09.005.

17. Olivati CA, Ferreira M, Carvalho AJF, Balogh DT, Oliveira Jr ON, von Seggern H, et al. Polymer light emitting devices with Langmuir-Blodgett (LB) films: Enhanced performance due to an electron-injecting layer of ionomers. *Chemichal Physics Letters*. 2005;408(1-3):31-36. DOI: 10.1016/j.cplett.2005.03.144.

18. Braunger ML, Barros A, Ferreira M, Olivati CA. Electrical and electrochemical measurements in nanostructured films of polythiophene derivatives. *Electrochimica Acta*. 2015;165:1-6. DOI: 10.1016/j.electacta.2015.02.232.

19. Nalwa HS, ed. *Handbook of Surfaces and Interfaces of Materials*. San Diego: Academic Press; 2001.

20. Lange U, Mirsky VM. Separated analysis of bulk and contact resistance of conducting polymers: Comparison of simultaneous two- and four-point measurements with impedance measurements. *Journal of Electroanalytical Chemistry*. 2008;622(2):246-251. DOI: 10.1016/j.jelechem.2008.06.013.

21. Salleo A. Charge transport in polymeric transistors. *Materials Today*. 2007;10(3):38-45. DOI: 10.1016/S1369-7021(07)70018-4.

22. Kline RJ, McGehee MD, Kadnikova EN, Liu J, Fréchet JMJ. Controlling the Field-Effect Mobility of Regioregular Polythiophene by Changing the Molecular Weight. *Advanced Materials*. 2003;15(18):1519-1522. DOI: 10.1002/adma.200305275.

23. Park YD, Kim DH, Jang Y, Cho JH, Hwang M, Lee HS, et al. Effect of side chain length on molecular ordering and field-effect mobility in poly(3-alkylthiophene) transistors. *Organic Electronics*. 2006;7(6):514-520. DOI: 10.1016/j.orgel.2006.07.007.

24. Li G, Shrotriya V, Huang J, Yao Y, Moriarty T, Emery K, et al. High-efficiency solution processable polymer photovoltaic cells by self-organization of polymer blends. *Nature Materials*. 2005;4:864-868. DOI: 10.1038/nmat1500.

25. Reitzel N, Greve DR, Kjaer K, Howes PB, Jayaraman M, Savoy S, et al. Self-Assembly of Conjugated Polymers at the Air/Water Interface. Structure and Properties of Langmuir and Langmuir-Blodgett Films of Amphiphilic Regioregular Polythiophenes. *Journal of the American Chemical Society*. 2000;122(24):5788-5800. DOI: 10.1021/ja9924501.